Complex emission dynamics of type-II GaSb/GaAs quantum dots

Kamil Gradkowski' , Nicola Pavarelli, Tomasz J. Ochalski, David P. Williams, Jun Tatebayashi, Guillaume Huyet, Eoin P. O'Reilly, and Diana L. Huffaker

Citation: Appl. Phys. Lett. **95**, 061102 (2009); doi: 10.1063/1.3202419

View online: http://dx.doi.org/10.1063/1.3202419

View Table of Contents: http://aip.scitation.org/toc/apl/95/6

Published by the American Institute of Physics

Complex emission dynamics of type-II GaSb/GaAs quantum dots

Kamil Gradkowski,[1,2,a)] Nicola Pavarelli,[1,2] Tomasz J. Ochalski,[1] David P. Williams,[1] Jun Tatebayashi,[3] Guillaume Huyet,[1,2] Eoin P. O'Reilly,[1,4] and Diana L. Huffaker[3]
[1]*Tyndall National Institute, Lee Maltings, Cork, Ireland*
[2]*Department of Applied Physics and Instrumentation, Cork Institute of Technology, Rossa Avenue, Cork, Ireland*
[3]*Department of Electrical Engineering and California Nano Systems Institute, University of California Los Angeles, California 90095, USA*
[4]*University College Cork, College Road, Cork, Ireland*

(Received 28 April 2009; accepted 21 July 2009; published online 10 August 2009)

Optical properties of the GaSb/GaAs quantum dot system are investigated using a time-resolved photoluminescence technique. In this type-II heterostructure the carriers of different species are spatially separated and, as a consequence, a smooth evolution of both the emission wavelength and decay timescale is observed. A wavelength shift of 170 nm is measured simultaneously with the progressive timescale change from 100 ps to 23 ns. These phenomena are explained by the evolution of the carrier density, which brings a modification to the optical transition probability as well as the shift in the emission toward the higher energies. © *2009 American Institute of Physics*.
[DOI: 10.1063/1.3202419]

Antimony-based compounds are promising materials since their combination with elements such as gallium, indium, or more complex alloys, such as dilute nitrides, will enable the realization of photonic materials for emission over a wide range of wavelengths in the infrared. For example, quinary InGaNAsSb quantum wells (QWs) grown lattice-matched to GaAs can be tuned to emit between 1.1 and 1.5 μm and above.[1] In quantum dot (QD) heterostructures, InSb is employed in midinfrared emitters (3–5 μm),[2] and GaSb shows potential for a wide range of applications in the telecommunications window.[3] The unique properties of GaSb/GaAs QDs make them a very interesting alternative to existing InAs/GaAs QD and dilute nitride QW technology.[4] The addition of Sb strongly affects the band alignments leading to the realization of type-II heterostructures such as GaSb/GaAs. Recent studies on similar materials include photoluminescence (PL) and photoreflectance of GaSb/GaAs QD[5,6] and time resolved PL (TRPL) of GaSb islands[7] and InAs/GaSbAs QDs.[8]

Unlike type-I InAs/GaAs QDs, the GaSb/GaAs QDs exhibit a type-II band alignment, where the holes are trapped in the dot, while the QD presents no confinement for the electrons. This leads to interesting physical phenomena as well as offering a freedom of band-gap engineering, because by capping the dots with various materials, a wide range of emission wavelengths can be achieved. In type-II structures the inherent carrier separation leads to a much lower wave function overlap than in type-I structures, and therefore the optical transition probability is expected to be lower. As a consequence, long radiative lifetimes are anticipated on the order of tens of nanoseconds.[9,10] The slow recombination rate means that the excited states can be populated easily, leading to the filling of the QD. The emission from higher excited states will contribute to the shift in the maximum of the emission wavelength toward the blue. This effect occurs at the same time as the shift caused by the Coulomb attraction between the carriers leading to the bending of the band. This brings the electrons closer to the QDs, forming a tight shell around the dot. This additionally increases the energy of the transition, which is a well-known feature of the type-II heterostructures,[9–12] but also increases the wave function overlap and therefore also the optical transition probability.[13,14] Overall, the emission dynamics of type-II QDs is a complex mechanism, where for a given carrier density, there will be a specific maximum of the emission wavelength with a specific recombination rate. During the course of the experiment, when the carrier density varies, several physical quantities will simultaneously vary, leading to an intricate temporal evolution of the system.

The structure under the experimental consideration was a molecular-beam-epitaxy grown structure of GaSb/GaAs QDs overgrown with an $In_{0.3}Ga_{0.7}As$ QW with a nominal thickness of 7 nm. The capping consisted of a 100 nm thick GaAs layer (Fig. 1). The dynamic properties of the GaSb/GaAs QDs have been investigated using a TRPL experiment. The structure was cooled down to 7 K and excited using a 780 nm PicoQuant pulsed laser diode. The PL was detected by a Hamamatsu streak camera system equipped with an infrared-enhanced thermoelectrically chilled photocathode. The results of TRPL measurements are presented in Fig. 2, where the color scale depicts the logarithm of the intensity of

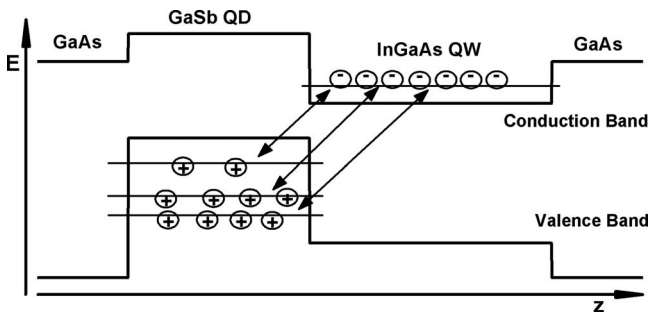

FIG. 1. Band alignment schematic of the GaSb/GaAs QD in the InGaAs QW. Main channels of radiative recombination, depicted as arrows, exist between the electrons in the QW and the holes on the QD levels.

a)Electronic mail: kamil.gradkowski@tyndall.ie.

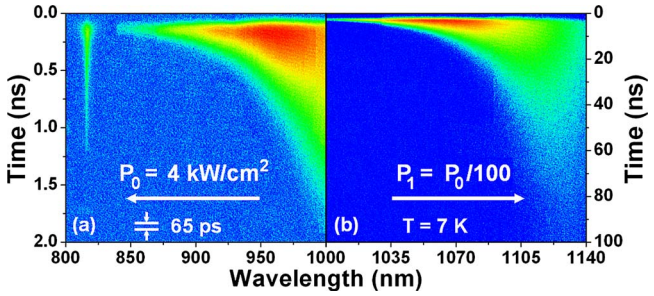

FIG. 2. (Color online) Streak images of the GaSb/GaAs QDs. (a) represents fast dynamic range under high-power excitation density, while (b) represents slow decay under low-power excitation density. The time axis for (a) is 20 times shorter than that for (b), to emphasize the different decay times observed under both conditions.

the emission as a function of both wavelength and time. In order to observe the emission dynamics at shortest wavelengths, we highly populated the dots using a high-power excitation density of P_0=4 kW/cm^2. In order to measure the fast decay rates observed in this regime, the streak camera was operated in the synchroscan mode with a repetition rate of 75.6 MHz, providing a temporal resolution by the 65 ps laser pulse. Figure 2(a) shows that the central emission wavelength suffers a redshift and the emission rate decreases with time. This indicates that the maximum emission wavelength and dipole moment depends strongly on the carrier density and to investigate the low carrier density regime, the streak camera was subsequently used in a slow-sweep mode operating at 1 MHz and the laser excitation power density was reduced to $P_1=P_0/100$. In such a case, the temporal resolution was limited by the streak image to 0.5 ns and shown on Fig. 2(b). For this low carrier density regime, the emission occurred up to 1140 nm and the decay rate decreased by two orders of magnitude.

By combining results obtained at low and high power excitation density, we observed a total redshift of 170 nm, corresponding to 193 meV and an increase in the decay time from 100 ps to 23 ns. This behavior is shown in Fig. 3, where we present the decay traces extracted from the streak images (Fig. 2) at different wavelengths. The specific timescales are summarized in Table I for both regimes of excitation in adjacent columns. The wavelengths around 1 μm were covered by both experimental modes and, therefore, we obtain decay data under different excitation power conditions. For the same wavelengths, nearly equal decays are observed for both experiments.

The strong variation in the decay time as a function of wavelength differs from that observed in conventional type-I InAs/GaAs QDs[15,16] where a single decay timescale, usually

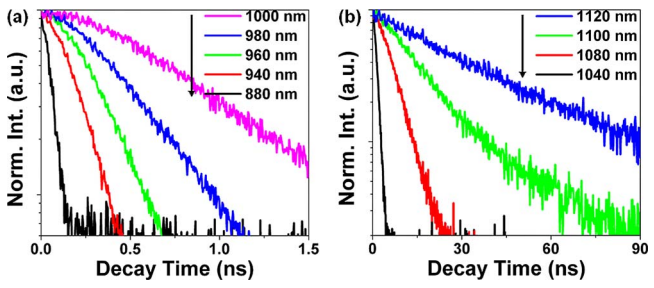

FIG. 3. (Color online) Decay traces for different emission wavelengths. Fast (a) and slow (b) dynamic ranges are shown.

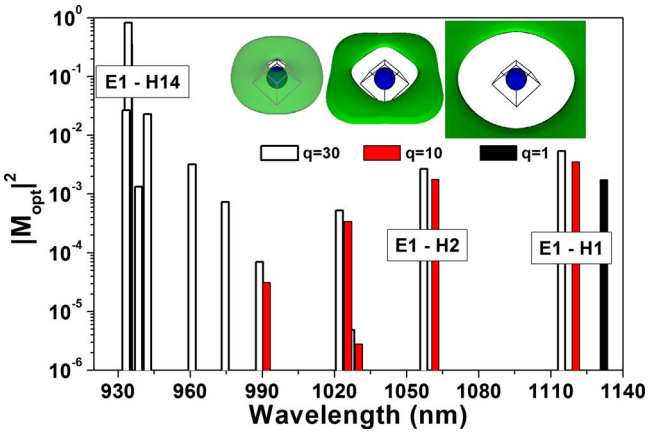

FIG. 4. (Color online) Self-consistent eight-band $\mathbf{k}\cdot\mathbf{p}$ calculations of the optical matrix element for a transition between the ground-state QW electron and the QD hole states as a dependence of the injected carrier density (q). The inset shows the ground-state and electron and hole wave functions for the presented charge densities.

on the order of a nanosecond, is observed for each energy level. For the structure investigated here, the holes are captured by the dot, while the electrons are filling the QW. As a natural consequence, the carriers are attracted to each other and the rearrangement of the charge density modifies the optical transition probability, as the electron wave function penetrates the QD and the overlap with the hole wave functions dramatically increases. With the depletion of carriers occurring during the radiative recombination process, the ring of electrons moves further away from the QD, as the reduced number of holes decreases the attractive potential. This in turn leads to a reduction in the wave function overlap and decrease in the optical matrix element. As a consequence the radiative recombination rate decreases.

To further investigate this point, we calculated the energy levels and wave functions using an 8-band $\mathbf{k}\cdot\mathbf{p}$ algorithm including self-consistent Coulomb interactions.[14] The material parameters for the calculations were taken from Ref. 17. The main results of these calculations are shown in Fig. 4, where the dipole moment associated with various transitions is shown for three different carrier densities corresponding to q=1, 10, and 30 electron-hole pair per dot. The inset shows electron and hole ground state wave functions for the three selected values of q. As was shown in Ref. 14, filling the dot leads to Coulomb repulsion of the holes, which increases their potential energy and blueshifts the spectrum. The largest value of q corresponds to the experimental situation immediately after a high power density excitation pulse where the hole concentration in the QD is at its highest. In such a case, the largest dipole moment is associated with the transition between the QW electron (E1) and the 14th hole energy level (H14) of Fig. 4. This is a direct consequence of Coulomb interaction that attracts the electrons toward the dot. The maximum overlap between the holes and electron wave function occurs for high order hole states with a substantial probability in the outer part of the dot. As a result, high order transitions such as E1-H14 will have a much faster decay rate at shorter wavelengths as experimentally observed in Figs. 2 and 3. As those states become depopulated, the maximum emission suffers a redshift

TABLE I. Decay times at different wavelengths for both dynamic ranges of the experiment.

Wavelength (nm)	880	920	960	1010	1020	1030	1060	1090	1120
Fast dynamic range τ (ns)	0.10	0.17	0.32	0.92	1.11	1.42	⋯	⋯	⋯
Slow dynamic range τ (ns)	⋯	⋯	⋯	0.78	1.15	1.30	3.11	8.88	23.08

and the decay time increases since lower states have a lower overlap with the electron states. With decreasing hole density, the effects of the Coulomb interaction become weaker, thus the electron-hole overlap and the redshift further decrease.

Experimentally, we observe a continuous shift rather than discrete transitions. This can be explained by the large effective mass of the holes and standard broadening resulting from dispersion in dot size and composition. For type-II dots, such as InAs/GaAsSb, where only the electrons are confined, one observes similar physics with discrete energy levels.[12]

In conclusion, we have carried out a detailed analysis of the complex emission dynamics of type-II GaSb/GaAs QDs, where we observe a simultaneous evolution of the emission wavelength and timescale. The overall dynamics of the emission of the GaSb/GaAs QDs is explained as a combination of carrier filling and Coulomb interaction. By increasing the carrier density within the dots, higher energy hole states have a stronger interaction with the electrons confined outside the dots thus leading to a fast decay of the blue part of the optical spectrum. Coulomb interaction between the electrons and the holes also increases the optical transition probability and contributes to the shift in the emission spectrum. These properties could be potentially useful in the design of high frequency optoelectronic devices operating at a wide range of wavelengths.

This work was supported by the European Union under Marie Curie Actions (Contract No. 041985), Science Foundation Ireland (Contract No. 06/RFP/ENE014) and by the Air Force Office of Scientific Research (Contract No. FA9550-06-1-0407) under Gernot Pomrenke and Kitt Rheinhardt. This research was conducted under the framework of the INSPIRE program, funded by the Irish Governement's Program for Research in Third Level Institutions, Cycle 4, National Development Plan 2007–20013.

[1] J. S. Harris, R. Kudrawiec, H. B. Yuen, S. R. Bank, H. P. Bae, M. A. Wistey, D. Jackrel, E. R. Pickett, T. Sarmiento, L. L. Goddard, V. Lordi, and T. Gugov, Phys. Status Solidi B **244**, 2707 (2007).
[2] O. G. Lyublinskaya, V. A. Solov'ev, A. N. Semenov, B. Ya. Meltser, Ya. V. Terent'ev, L. A. Prokopova, A. A. Toropov, A. A. Sitnikova, O. V. Rykhova, S. V. Ivanov, K. Thonke, and R. Sauer, J. Appl. Phys. **99**, 093517 (2006).
[3] C. Mourad, D. Gianardi, and R. Kaspi, J. Appl. Phys. **88**, 5543 (2000).
[4] H. P. Bae, S. R. Bank, H. B. Yuen, T. Sarmiento, E. R. Pickett, M. A. Wistey, and J. S. Harris, Appl. Phys. Lett. **90**, 231119 (2007).
[5] J. Tatebayashi, A. Khoshakhlagh, S. H. Huang, G. Balakrishnan, L. R. Dawson, D. L. Huffaker, D. A. Bussian, H. Htoon, and V. Klimov, Appl. Phys. Lett. **90**, 261115 (2007).
[6] K. Gradkowski, T. J. Ochalski, D. P. Williams, J. Tatebayashi, A. Khoshakhlagh, G. Balakrishnan, E. P. O'Reilly, G. Huyet, L. R. Dawson, and D. L. Huffaker, J. Lumin. **129**, 456 (2009).
[7] S. Horst, S. Chatterjee, K. Hantke, P. J. Klar, I. Nemeth, W. Stolz, K. Volz, C. Bückers, A. Thränhardt, S. W. Koch, W. Rühle, S. R. Johnson, J.-B. Wang, and Y.-H. Zhang, Appl. Phys. Lett. **92**, 161101 (2008).
[8] W.-H. Chang, Y.-A. Liao, W.-T. Hsu, M.-C. Lee, P.-C. Chiu, and J.-I. Chyi, Appl. Phys. Lett. **93**, 033107 (2008).
[9] L. Shterengas, R. Kaspi, A. P. Ongstad, S. Suchalkin, and G. Belenky, Appl. Phys. Lett. **91**, 101106 (2007).
[10] C.-K. Sun, G. Wang, J. E. Bowers, B. Brar, H.-R. Blank, H. Kroemer, and M. H. Pilkuhn, Appl. Phys. Lett. **68**, 1543 (1996).
[11] F. Hatami, N. N. Ledenstov, M. Grundmann, J. Böhrer, F. Heinrichsdoff, M. Beer, D. Bimberg, S. S. Ruvimov, P. Werner, U. Gösele, J. Heydenreich, U. Richter, S. V. Ivanov, B. Y. Meltser, P. S. Kop'ev, and Z. I. Alferov, Appl. Phys. Lett. **67**, 656 (1995).
[12] Y.-A. Liao, W.-T. Hsu, P.-C. Chiu, J.-I. Chyi, and W.-H. Chan, Appl. Phys. Lett. **94**, 053101 (2009).
[13] J. R. Madureira, M. P. F. de Godoy, M. J. S. P. Brasil, and F. Iikawa, Appl. Phys. Lett. **90**, 212105 (2007).
[14] K. Gradkowski, T. J. Ochalski, D. P. Williams, S. B. Healy, J. Tatebayashi, G. Balakrishnan, E. P. O'Reilly, G. Huyet, and D. L. Huffaker, Phys. Status Solidi B **246**, 752 (2009).
[15] L. Ya. Karachinsky, S. Pellegrini, G. S. Buller, A. S. Shkolnik, N. Yu. Gordeev, V. P. Evtikhiev, and V. B. Novikov, Appl. Phys. Lett. **84**, 7 (2004).
[16] B. L. Liang, Zh. M. Wang, Yu. I. Mazur, and G. J. Salamo, Appl. Phys. Lett. **89**, 243124 (2006).
[17] I. Vurgaftman, J. R. Meyer, and L. R. Ram-Mohan, J. Appl. Phys. **89**, 5815 (2001).